Biochemistry and Biophysics Reports 28 (2021) 101137

Contents lists available at ScienceDirect

Biochemistry and Biophysics Reports

journal homepage: www.elsevier.com/locate/bbrep

Probing TGF-β1-induced cytoskeletal rearrangement by fluorescent-labeled silica nanoparticle uptake assay

HyeRim Shin, Jun-Hyuk Choi, Ji Youn Lee *

Biometrology Group, Division of Chemical and Biological Metrology, Korea Research Institute of Standards and Science, 267 Gajeong-ro, Yuseong-gu, Daejeon, 34113, Republic of Korea

ARTICLE INFO

Keywords:
Cytoskeletal rearrangement
Flow cytometry
Fluorescent-labeled silica nanoparticle
HaCaT cell
TGF-β1

ABSTRACT

Cytoskeletal proteins are essential in maintaining cell morphology, proliferation, and viability as well as internalizing molecules in phagocytic and non-phagocytic cells. Orderly aligned cytoskeletons are disturbed by a range of biological processes, such as the epithelial–mesenchymal transition, which is observed in cancer metastasis. Although many biological methods have been developed to detect cytoskeletal rearrangement, simple and quantitative *in vitro* approaches are still in great demand. Herein, we applied a flow cytometry-based nanoparticle uptake assay to measure the degree of cytoskeletal rearrangement induced by transforming growth factor β1 (TGF-β1). For the assay, silica nanoparticles, selected for their high biocompatibility, were fluorescent-labeled to facilitate quantification with flow cytometry. Human keratinocyte HaCaT cells were treated with different concentrations of TGF-β1 and then exposed to FITC-labeled silica nanoparticles. Increasing concentrations of TGF-β1 induced gradual changes in cytoskeletal rearrangement, as confirmed by conventional assays. The level of nanoparticle uptake increased by TGF-β1 treatment in a dose-dependent manner, indicating that our nanoparticle uptake assay can be used as a quick and non-destructive approach to measure cytoskeletal rearrangement.

1. Introduction

The cytoskeleton is a complex filament bundle that plays a pivotal role in maintaining cell structure and communication between neighboring cells, as well as cell migration, invasion, and the metastasis of tumor cells [1–3]. Orderly aligned cytoskeletons are disturbed by different biological processes, such as the epithelial-to-mesenchymal transition (EMT). The EMT is a change from tightly connected cells to highly motile mesenchymal cells that occurs during cellular development; this process also participates in cell migration, invasion, and the metastasis of tumor cells [4–7]. Wound healing (or wound re-epithelialization) is another biological phenomenon where active cytoskeletal rearrangement occurs. Both EMT and wound healing involve the disruption of adherens junctions leading to the induction of cell migration by growth factors [8]. Many studies have investigated various inhibitors or stimulators of cytoskeletal proteins in order to observe how these substances affect cell morphology and their further influence on cell migration and invasion [9–12]. Such research has typically employed traditional assays such as Western blot, PCR, and optical microscopy, most of which are end-point and destructive, as well as relatively time-consuming. The introduction of new analytical methods with simple, rapid, and non-destructive properties could greatly aid the understanding of cytoskeletal rearrangement.

Nanoparticles possess advantages including a large surface to volume ratio and a facilitated uptake by cells due to their small size [13], features that have encouraged their use in diverse fields such as drug delivery for advanced therapy and diagnosis [14,15], the food industry [16], and cosmetics [17] over recent decades. In particular, nanoparticles have been chosen for various therapeutic purposes due to the benefits they provide as drug carriers [18,19], such as facile delivery into cells and their targeting ability using surface modification. Fluorescent-labeling can further improve the usability of nanoparticles due to the selectivity, good contrast, and wide range of possible molecules it provides; indeed, fluorescent-labeled nanoparticles are considered as ideal candidates for cancer diagnosis for their high sensitivity and relatively inexpensive techniques [20]. Among different

Abbreviations: TGF-β1, transforming growth factor β1; EMT, epithelial–mesenchymal transition; FCM, flow cytometry; FITC-SiO_2NPs, FITC-labeled silica nanoparticles.

* Corresponding author.
E-mail address: jylee@kriss.re.kr (J.Y. Lee).

https://doi.org/10.1016/j.bbrep.2021.101137
Received 21 July 2021; Received in revised form 31 August 2021; Accepted 15 September 2021

nanomaterials, silica nanoparticles are employed in diverse applications for their low cytotoxicity, stability, and ease of production [21–23].

In this study, we employed fluorescent-labeled silica nanoparticles as a tool for detecting cytoskeletal rearrangement in an immortalized keratinocyte cell line, HaCaT. We chose HaCaT as a model cell line because the skin is the organ that is primarily exposed to nanoparticles along with the lungs, intestines, and blood, and it is often used to study EMT [24–26]. First, we induced cytoskeletal rearrangement by various chemical treatments and chose the appropriate stimulator by investigating morphological changes and nanoparticle uptake. We then applied our previously developed quantitative assay, which measured fluorescently labeled nanoparticle uptake in mammalian cells using a flow cytometer [27]. In that work, we demonstrated the assay with different types of cells and showed that the cellular uptake of nanoparticles is largely proportional to cell area. Since cytoskeletal rearrangement is accompanied by changes in the area of cell adhesion, we anticipate that the nanoparticle uptake assay may provide a means to indirectly probe the cytoskeletal rearrangement of keratinocytes.

2. Materials and methods

2.1. Cell culture

Human keratinocyte HaCaT cells were obtained from the Korean Cell Line Bank. Cells were maintained in DMEM supplemented with 10% FBS and 1% penicillin-streptomycin at 37 °C under 5% CO_2 atmosphere. Analyzing cell viability by trypan blue exclusion was performed with a Countess II Automated Cell Counter (Invitrogen). All culture supplies and reagents were obtained from Thermo Fisher Scientific, unless otherwise indicated.

2.2. Chemicals and nanoparticle treatment

To choose an appropriate stimulant for the cytoskeletal rearrangement, various chemicals at fixed concentrations—TGF-β1 (2 ng/mL), Y27632 (10 μM, Enzo Life Sciences), and blebbistatin (25 μM, Enzo Life Sciences)—were treated to HaCaT cells in culture. After the selection process, cells were treated with a two-fold serial dilution of TGF-β1 (0, 0.5, 1, 2, 4 ng/mL) for 5 days. During the prolonged treatment of TGF-β1, cells were subcultured every other day to avoid over-confluence. After the treatment, cells were removed from the culture dish and subcultured in a 6-well plate at a density of 2×10^5 cells per well. After 24 h, cells were washed with fresh media to remove residual TGF-β1 and incubated with different concentrations of nanoparticle solutions that were prepared in the culture media. We used in-house synthesized fluorescein 5(6)-isothiocyanate (FITC)-labeled SiO_2 nanoparticles (FITC-SiO_2NPs) of 25 nm size as described in our previous study [27]. FITC-labeled polystyrene nanoparticles of 20 nm size were purchased from Nanocos. After the nanoparticle treatment for 24 h, cells were washed twice with 1x PBS to remove residual nanoparticles, and then cells were prepared with trypsinization for flow cytometry (FCM) analysis.

2.3. Flow cytometry analysis

FCM data was obtained using a FACSVerse™ (BD Biosciences) and analyzed with FlowJo (version X, FlowJo LLC). For data reliability, a large number of cells (>20,000 events) were recorded in the acquisition step. In brief, a main cell population was selected to exclude debris, and then a single-cell population was gated in the scatter plot. Histograms in the FITC channel for the single-cell population were analyzed. The background signal in the FITC channel of each sample without nanoparticle treatment was subtracted from the measured value of each sample after nanoparticle treatment.

2.4. Bright-field and fluorescence imaging

Cell images in bright-field were obtained using an inverted microscope (Olympus IX71). To visualize and analyze the location and distribution of the nanoparticles in cells, cells were fixed with 4% paraformaldehyde and 0.1% Triton X-100 for 2 min, and then post-fixed with 4% paraformaldehyde for 15 min. Actin was stained with rhodamine-conjugated phalloidin for 30 min at room temperature and then the nuclei were counterstained with 4,6-diamidino-2-phenylindole (DAPI) for 5 min. ProLong® Gold antifade reagent was used for mounting coverslips. Cells were imaged with either a Z1 microscope with ApoTome 2 or an LSM 810 confocal microscope (ZEISS). All image analyses, such as cell number count and area calculations, were performed with ImageJ (version 1.52a, NIH).

2.5. Western blot analysis

Cells were lysed in ice-cold 2x Laemmli sample buffer (0.125 M Tris-HCl, 20% glycerol, 4% sodium dodecyl sulfate, and 0.004% bromophenol blue) with protease inhibitor cocktail (Sigma-Aldrich). The cell lysates were separated by SDS-PAGE and transferred to a 0.2 μm nitrocellulose membrane. The membrane was probed with primary antibody, E-cadherin (BD Biosciences, 610181, 1: 1000), N-cadherin (Abcam, ab18203, 1: 500), Fibronectin (BD Biosciences, 610077, 1:1000), and α-tubulin (Sigma- Aldrich, T5168, 1: 1000). Primary antibodies were detected with peroxidase-conjugated AffiniPure goat anti-mouse IgG or goat anti-rabbit IgG (Jackson ImmunoResearch Laboratories) at 1:2000 dilution, and visualized by enhanced chemiluminescence.

2.6. Statistical analysis

Experiments were independently repeated at least in triplicate. Error bars in the graphical data represent standard deviations. A two-tailed *t*-test was used for statistical analysis in Excel 2016 (Microsoft), and statistical significance was claimed when the p-value was lower than 0.05. In figure legends, asterisks denote statistically significant differences between conditions and treatments (*$p < 0.05$, **$p < 0.01$, ***$p < 0.005$, and ns: not significant).

3. Results and discussion

3.1. Selection of an appropriate stimulator for HaCaT cells

The main purpose of this study was to design a method to apply the nanoparticle uptake assay to the measurement of cytoskeletal change in epidermal keratinocytes using fluorescent-labeled nanoparticles. We tested three cytoskeleton modifiers, namely EMT inducer TGF-β1, Rho kinase inhibitor Y27632, and myosin II inhibitor blebbistatin, to explore the assay development, along with dimethyl sulfoxide (DMSO)-treated cells as a control. HaCaT cells were treated with the modifiers and then exposed to FITC-SiO_2NPs. Upon treatment with TGF-β1, cells lost their tight junctions and exhibited a mesenchymal-like appearance, as shown in the brightfield micrograph in Fig. S1A. On the other hand, cells treated with Y27632 and blebbistatin showed loosened cell–cell contacts with spike formations. Among the treatments, TGF-β1-treated cells showed the biggest change in FITC intensity compared to control and other samples in the FCM analysis (Fig. S1B). A higher level of nanoparticle uptake by TGF-β1-treated cells was also confirmed with fluorescence microscopy, showing the presence of nanoparticles near the nuclei (Fig. S1A). Overall, TGF-β1-treated cells showed both a dramatic change in morphology and an increased nanoparticle uptake compared to cells treated with either Y27632 or blebbistatin. Therefore, in the following sections, we use TGF-β1 to induce cytoskeletal rearrangement.

Next, we checked whether the addition of nanoparticles induces noticeable changes in HaCaT cells. Within the concentration range tested, 0–50 μg/mL FITC-SiO_2NPs, cellular proliferation and

morphology remained unchanged in both untreated and TGF-β1-treated cells (Fig. 1A). For the FCM analysis, single cells were gated (Fig. S2) and FITC channel histograms were compared (Fig. 1B and C). Compared to untreated cells, TGF-β1-treated cells showed a significant increase in the FITC intensity of HaCaT cells at both 10 and 50 μg/mL nanoparticle concentrations. In the case of cells treated with 50 μg/mL nanoparticles, a much higher FITC intensity change was induced by the TGF-β1 treatment; however, the fold-increase was similar to the cells treated with 10 μg/mL nanoparticles. Accordingly, both concentrations seemed suitable for investigating cytoskeletal changes.

3.2. Analyses of HaCaT cells treated with increasing concentrations of TGF-β1

When HaCaT cells are treated with an appropriate concentration of TGF-β1, a change known as the EMT occurs [7,24]. In the EMT, the morphology of cells typically changes, spreading them out and thus increasing the adhesion area of the cells. It has been documented that epithelial cell morphology and protein expression levels switch to show mesenchymal-like features by treatment with TGF-β1 in a concentration-dependent manner [28,29]. In terms of the nanoparticle uptake assay, we anticipated that HaCaT cells treated with increasing concentrations of TGF-β1 would show a gradual change in cellular status, and that such changes could be probed quantitatively. The phenotypic changes in HaCaT cells by increasing concentrations of TGF-β1 were first analyzed by conventional methods, optical microscopy and Western blot, and then by the nanoparticle uptake assay.

HaCaT cells were treated for 5 days in two-fold serial concentrations of TGF-β1 ranging from 0 to 4 ng/mL. As the TGF-β1 concentration increased, strong cell–cell adhesion started to loosen and the area per cell increased, as shown in the micrographs and image analysis results in Fig. 2A and B. In the Western blot analysis, we monitored three adherens proteins, E-cadherin, N-cadherin, and fibronectin. Cadherins are one of major adhesion molecules forming adherens junctions in epidermal and

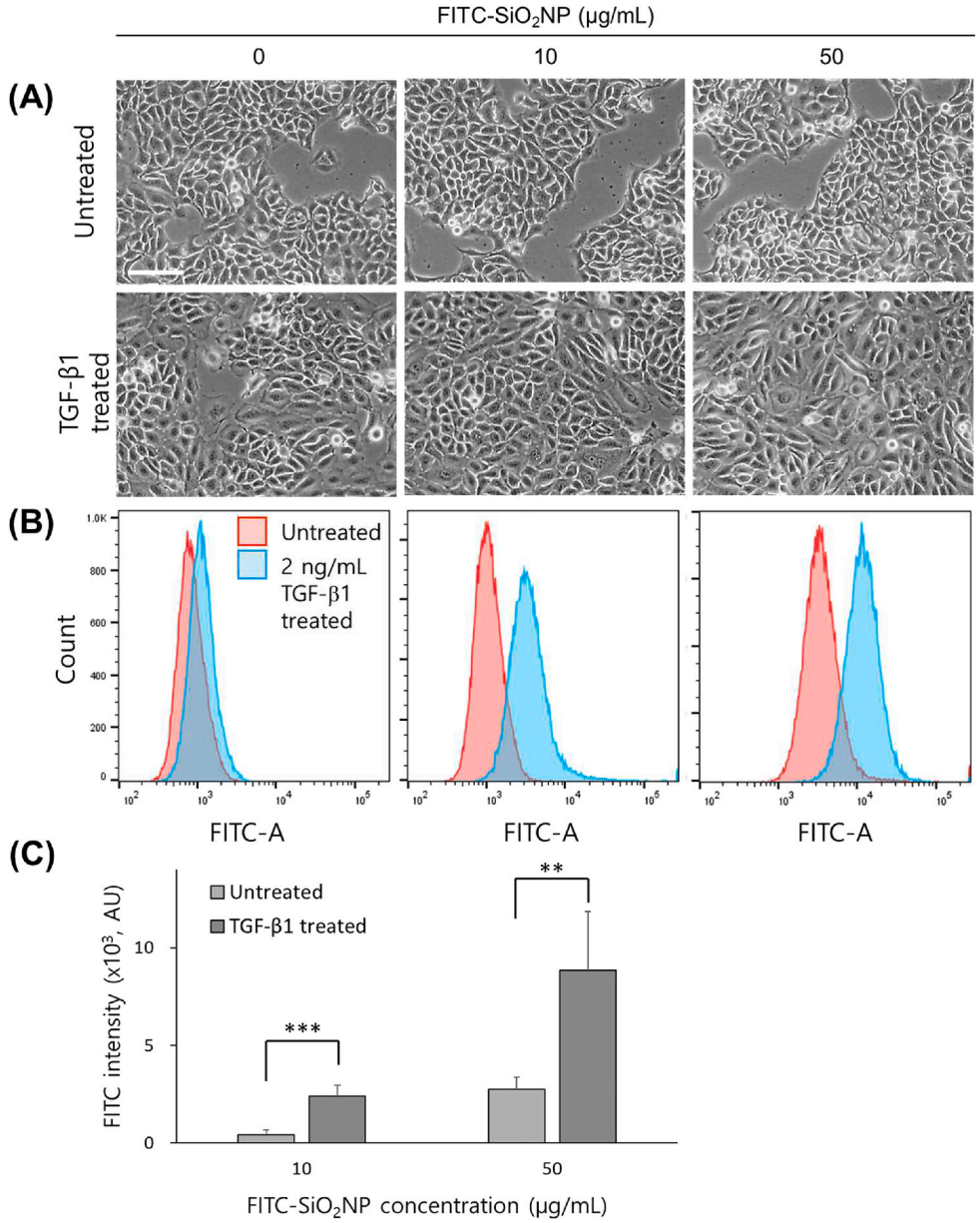

Fig. 1. HaCaT cells after the treatment of different concentrations of FITC-SiO_2NPs. (A) Micrographs showing morphological differences between untreated and 2 ng/mL TGF-β1-treated HaCaT cells. Scale bar = 100 μm. (B) Histogram shift of HaCaT cells in the FITC channel by the uptake of FITC-SiO_2NPs. (C) Bar graph showing the FITC intensity change of HaCaT cells by the uptake of FITC-SiO_2NPs.

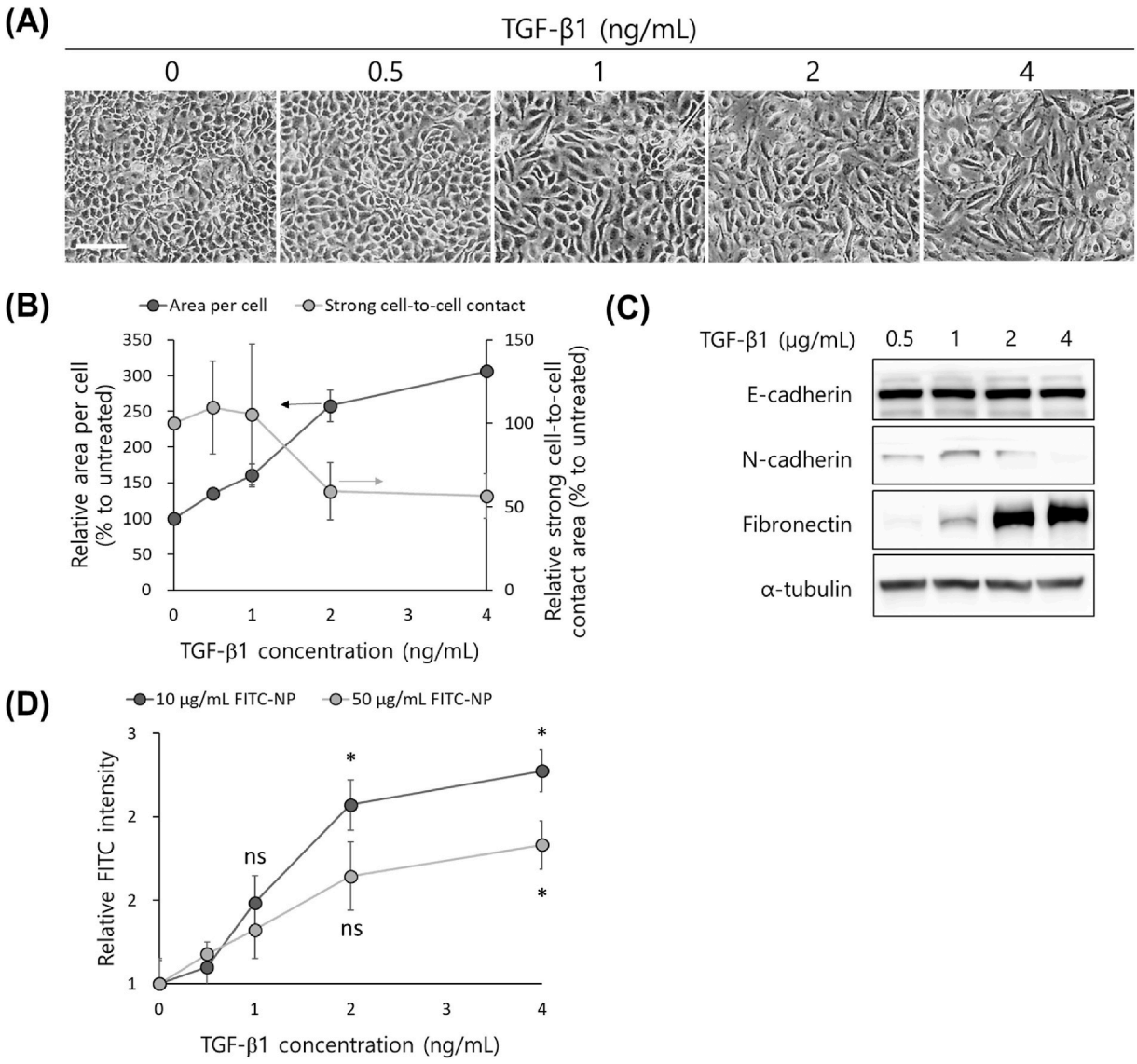

Fig. 2. Morphology and nanoparticle uptake changes by increasing concentrations of TGF-β1. (A) Brightfield images of HaCaT cells at day 5, showing morphological changes by TGF-β1 treatment. Scale bar = 100 μm. (B) Image analysis results of cell area and strong cell-to-cell contact area. (C) Western blot results at day 5 for a few adherens proteins indicative of the EMT. (D) Nanoparticle uptake assay results showing increased FITC intensity correlated with TGF-β1concentration.

epithelial cells [30]. E-cadherins are replaced by N-cadherins with a reorganized actin cytoskeleton followed by increased migratory characteristics from TGF-β1 treatment [28,31,32]. High levels of fibronectin are stimulated by TGF-β1 treatment, which lead cells to become motile and loosen their cell–cell contacts [33,34]. Protein immunoblot data showed that TGF-β1 treatment resulted in a slight decrease of E-cadherin expression, whereas a proportional increase of N-cadherin and fibronectin were observed with increasing concentrations of TGF-β1 (Fig. 2C and Fig. S3). Similar results were observed in HaCaT cells treated with TGF-β1 for 3 days, as presented in the Supplementary Information Fig. S3 along with brightfield images. In particular, the difference in expression level was remarkable in fibronectin: the sample treated with 4 ng/mL TGF-β1 showed a 30 times stronger band intensity than that of the sample treated with 0.5 ng/mL TGF-β1 for 5 days. Also, retarded cell proliferation (Fig. S4) with increasing concentrations of TGF-β1 was also observed, as reported previously [7,24]. These observations are typical phenotypic changes caused by the EMT, indicating that TGF-β1 effectively induces cytoskeletal rearrangement and influences cell proliferation. In sum, we were able to probe TGF-β1-mediated EMT responses in HaCaT cells, demonstrating that this system can be used with the nanoparticle uptake assay as an alternative way to probe cytoskeletal rearrangement and in turn the EMT process.

The nanoparticle uptake assay was performed on HaCaT cells, with the results summarized in Fig. 2D. The FITC intensity of the HaCaT cells increased in a TGF-β1 concentration-dependent manner with both 10 and 50 μg/mL FITC-SiO_2NPs, showing a steady intensity increase up to 2 ng/mL TGF-β1 concentration and then flattening. Although the absolute value of FITC intensity was much higher at 50 μg/mL FITC-SiO_2NPs (Fig. S5), the relative increase of FITC intensity was higher with 10 μg/mL FITC-SiO_2NPs. Even at the lowest tested TGF-β1 concentration (0.5 ng/mL), a noticeable uptake increase was observed (Fig. 2D). Given that the conventional assays indicated that cytoskeletal rearrangement occurs in TGF-β1 treated HaCaT cells in a concentration-dependent manner, a gradual increase in the level of nanoparticle uptake can probe the rearrangement. Increases in the FITC signal are expected to be attributable to two main factors. One is an increase of nanoparticle uptake possibly due to the increased cell-covered area by cytoskeletal rearrangement, and the other is a reduction of intracellular nanoparticle dilution by cell division due to the retarded cell proliferation. Elucidation of the relative contribution of these two factors or other possible

factors influencing nanoparticle uptake could follow in another study.

One thing to consider when applying this assay is that cytoskeleton disruption may occur when cells are exposed to nanoparticles, depending on the physicochemical properties, size, and exposure time [35,36]. For this reason, the choice of nanoparticle and experimental conditions such as concentration should be optimized. Under the experimental conditions that we adopted, the cytoskeleton was not adversely affected by the nanoparticle treatment. Based on the data so far, we concluded that cytoskeletal rearrangement can be probed quantitatively by the nanoparticle uptake assay in a minimally destructive manner and that the analyzed cells can be further analyzed with proper tools.

We then explored the nanoparticle uptake dynamics of the HaCaT cells. In most nanoparticle uptake experiments, 24 h is the common choice because it is a sufficient time for nanoparticle uptake while also short enough to avoid undesirable dilution effects from cell division [37]. However, shorter analysis times achieving a similar level of quantification would be preferred since the dilution effect by cell division can be lessened with shorter assay times. We measured the FITC intensity of cells at 2, 4, and 6 h. FITC intensity started to separate at the early time point of 2 h, after which the intensity plots further deviated at 4 and 6 h time points, showing a dose-dependent pattern (Fig. S6). From these data, we determined that the phenotypic differences can be probed with shorter nanoparticle incubation times than those in conventional nanoparticle uptake experiments.

To confirm that this *in vitro* analysis is not limited to the particular in-house synthesized silica nanoparticles employed here, we performed the same experiment with commercially available FITC-labeled polystyrene nanoparticles, 20 nm in size. An increase in FITC intensity was found, and FCM analysis supported that it was dependent on increasing TGF-β1 concentration (Fig. S7). Therefore, we emphasize that commercially available FITC-labeled nanoparticles are also applicable to this method.

3.3. Cellular morphology and nanoparticle localization

Further investigations into the structural changes of TGF-β1-treated

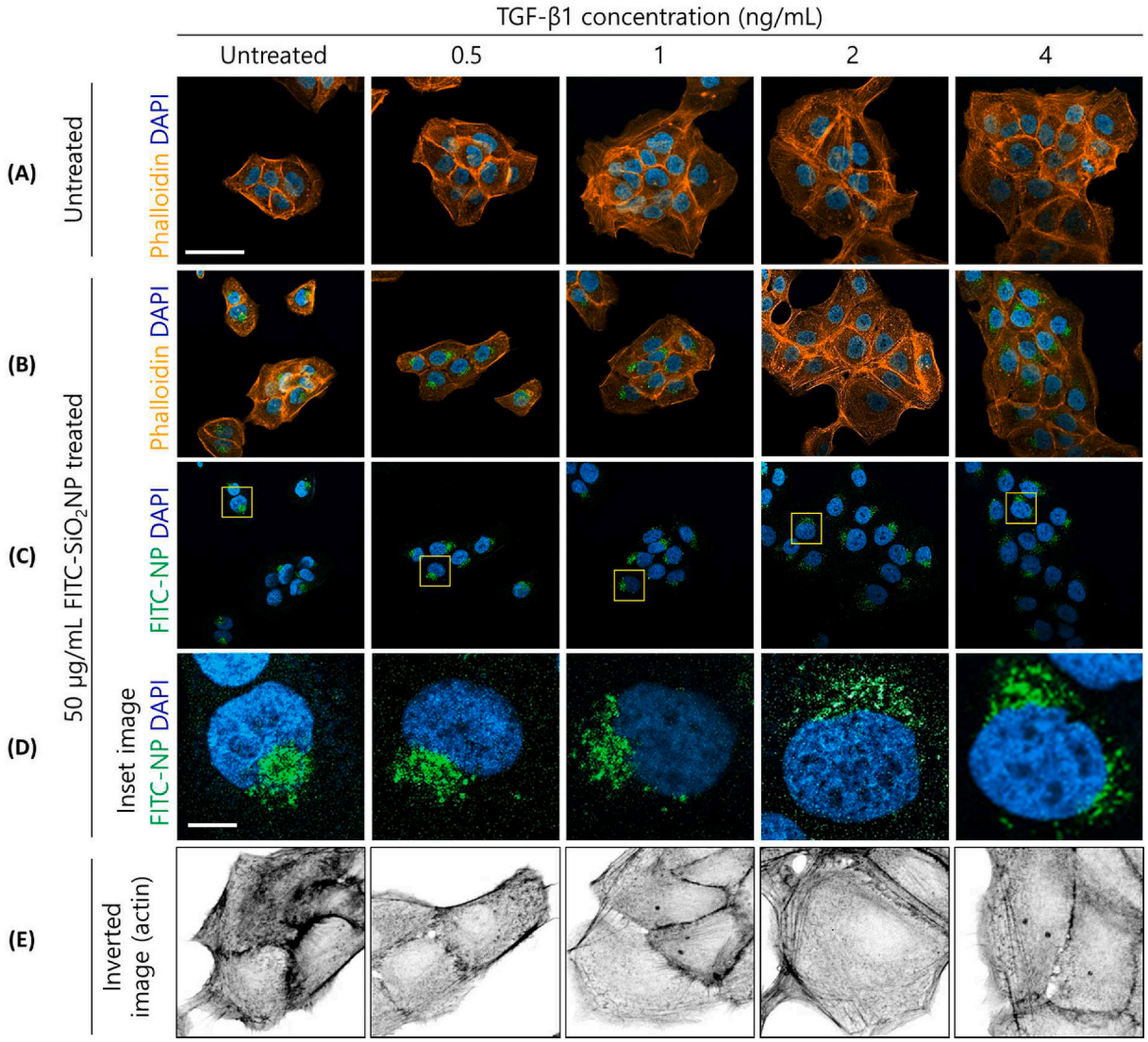

Fig. 3. Immunofluorescence staining and image analysis of HaCaT cells treated with increasing concentrations of TGF-β1. TGF-β1-treated HaCaT cells were stained with phalloidin (orange) and DAPI (blue), and show internalized FITC-SiO_2NPs (green). Merged images of phalloidin and DAPI co-staining are shown. (A) Untreated cells. Scale bar = 50 μm. (B) 50 μg/mL FITC-SiO_2NP treated cells. (C) Merged images of DAPI and FITC-SiO_2NP treated cells showing the location of the nanoparticles. The yellow boxes are highlighted areas of single nuclei with FITC-SiO_2NPs, enlarged in (D) Scale bar = 10 μm. (E) Inverted gray images of the phalloidin-staining images in (B) showing the structural changes of the actin filaments. (For interpretation of the references to colour in this figure legend, the reader is referred to the Web version of this article.)

HaCaT cells were performed via phalloidin staining to observe the actin arrangement and the localization of nanoparticles in the cells. In Fig. 3, the actin and the nucleus are stained orange and blue, respectively, and the nanoparticles appear green. The arrangement of actin changes along with the treated concentrations of TGF-β1. In the case of control HaCaT cells, actin was tightly ordered to form the rigid outer structure of the cells. When the cells were treated with TGF-β1, they displayed a motile phenotype: actin was rearranged (stretched) into filaments to form a filopodium [7,28,38]. As Liarte et al. reported in their study investigating the response of HaCaT cells to sustained TGF-β1 exposure [39], we also observed a spindle-shaped phenotype in the present work. To make the actin filaments more visible, inverted gray images of cropped sections of the phalloidin staining were obtained (Fig. 3E). As the concentration of treated TGF-β1 increased, more long-stretched actin filaments were observed with increasing lengths. The unit cell area also increased with increasing concentrations of TGF-β1, reaching a maximum at the 2 ng/mL TGF-β1 concentration, which is in good agreement with the brightfield image data presented in Fig. 2B.

Interestingly, the intracellular distribution of nanoparticles was also altered with TGF-β1 treatment. Most of the FITC-SiO_2NPs in the untreated cells were localized at a single spot near the nucleus, while increasing concentrations of TGF-β1 caused scattered nanoparticles throughout the cells (Fig. 3D). Given that nanoparticles accumulate in lysosomes before removal from cells [40], and lysosome distribution is closely related with the cytoskeleton [41], it is possible that cytoskeletal rearrangement also contributed to the change in nanoparticle localization.

In this article, we established an assay to detect cytoskeletal rearrangement by employing FITC-SiO_2NP uptake analysis with FCM. TGF-β1 was chosen to induce cytoskeletal rearrangement, which is an essential step in the EMT process, in epidermal keratinocyte HaCaT cells. Gradual phenotypic changes by increasing concentrations of TGF-β1 were confirmed by conventional assays. We found that the level of nanoparticle uptake increased in TGF-β1-treated cells in a concentration-dependent manner. We expect that the nanoparticle uptake increases due to the increased adhered cell area by TGF-β1 treatment, as we previously observed a linear relationship between cell area and nanoparticle uptake in various types of cells. We note that other biological causes for the increased nanoparticle uptake may also play a role. Also, the developed assay needs to be further validated with other cell types to be established as a reliable method to assess cytoskeletal rearrangement. We reserve additional investigations for future work.

Although the relationship between cytoskeletal rearrangement and nanoparticle uptake is not direct, since it shows a phenomenological correlation, we expect that the nanoparticle uptake assay can be utilized as a quantitative method for probing cytoskeletal rearrangement. In other words, while changes in nanoparticle uptake alone cannot probe the EMT process or cytoskeletal rearrangement, the experimental process in this work is simple and non-destructive, and the results are quantitative and readily comparable with different sets of experiments because the fluorescence values can be normalized with calibration beads. Because conventional assays to quantify EMT, such as Western blot analysis, immunocytochemistry, and PCR, are more qualitative and destructive analyses where cells are lysed or fixed, our assay can provide a valuable complement because the cells can be re-used for other downstream analyses. In addition, due to the multiplexed analysis capability of FCM, richer information can be obtained by analyzing cellular statuses, such as cell proliferation and marker expressions, together. To elucidate the relationship between nanoparticle uptake and cytoskeletal rearrangement, employment of diverse experimental platforms could be beneficial. For example, Rao et al. employed tension gauge tether and reflective interference contrast microscopy to probe cytoskeletal rearrangement [42]. They successfully probed and quantified the rearrangement to demonstrate that EGFR stimulation modulates the mechanical tension thresholds. Quantitative assessment of actin rearrangement can also be achieved by using antibodies for arginylated actin as introduced by Karakozova et al. [43] We envision that our assay will support conventional assays as an orthogonal method for probing cytoskeletal rearrangement.

Declaration of competing interest

Authors have declared no conflict of interest.

Acknowledgements

This work was supported by the Nano Material Technology Development Program (No. 2016M3A7B6908929) of the National Research Foundation and KRISS-GP2020-0003 from the Korea Research Institute of Standards and Science from the Ministry of Science and ICT.

Appendix A. Supplementary data

Supplementary data to this article can be found online at https://doi.org/10.1016/j.bbrep.2021.101137.

References

[1] P. Hotulainen, P. Lappalainen, Stress fibers are generated by two distinct actin assembly mechanisms in motile cells, J. Cell Biol. 173 (2006) 383–394.
[2] A. Hall, The cytoskeleton and cancer, Canc. Metastasis Rev. 28 (2009) 5–14.
[3] J. Shankar, I.R. Nabi, Actin cytoskeleton regulation of epithelial mesenchymal transition in metastatic cancer cells, PloS One 10 (2015) 1–12.
[4] J. Massagué, TGFβ in cancer, Cell 134 (2008) 215–230.
[5] D.S. Micalizzi, S.M. Farabaugh, H.L. Ford, Epithelial-mesenchymal transition in cancer: parallels between normal development and tumor progression, J. Mammary Gland Biol. Neoplasia 15 (2010) 117–134.
[6] S. Lamouille, J. Xu, R. Derynck, Molecular mechanisms of epithelial-mesenchymal transition, Nat. Rev. Mol. Cell. Biol. 15 (2014) 178–196.
[7] J. Xu, S. Lamouille, R. Derynck, TGF-B-induced epithelial to mesenchymal transition, Cell Res. 19 (2009) 156–172.
[8] D. Haensel, X. Dai, Epithelial-to-mesenchymal transition in cutaneous wound healing: where we are and where we are heading, Dev. Dynam. 247 (2018) 473–480.
[9] S. Even-Ram, et al., Myosin IIA regulates cell motility and actomyosin-microtubule crosstalk, Nat. Cell Biol. 9 (2007) 299–309.
[10] N.B. Wolf, et al., Influences of opioids and nanoparticles on *in vitro* wound healing models, Eur. J. Pharm. Biopharm. 73 (2009) 34–42.
[11] M.E. Grady, et al., Intracellular nanoparticle dynamics affected by cytoskeletal integrity, Soft Matter 13 (2017) 1873–1880.
[12] H.R. Shin, D. Kim, D.M. Helfman, Tropomyosin isoform Tpm2.1 regulates collective and amoeboid cell migration and cell aggregation in breast epithelial cells, Oncotarget 8 (2017) 95192–95205.
[13] R.A. Petros, J.M. Desimone, Strategies in the design of nanoparticles for therapeutic applications, Nat. Rev. Drug Discov. 9 (2010) 615–627.
[14] Z. Cheng, A. Al Zaki, J.Z. Hui, V.R. Muzykantov, A. Tsourkas, Multifunctional nanoparticles: cost versus benefit of adding targeting and imaging capabilities, Science 338 (2012) 903–910.
[15] S.C. Baetke, T. Lammers, F. Kiessling, Applications of nanoparticles for diagnosis and therapy of cancer, Br. J. Radiol. 88 (2015).
[16] P. Sanguansri, M.A. Augustin, Nanoscale materials development - a food industry perspective, Trends Food Sci. Technol. 17 (2006) 547–556.
[17] S. Raj, S. Jose, U.S. Sumod, M. Sabitha, Nanotechnology in cosmetics: opportunities and challenges, J. Pharm. BioAllied Sci. 4 (2012) 186–193.
[18] L. Huang, J. Wang, S. Huang, F. Siaw-debrah, Biochemical and Biophysical Research Communications Polyacrylic acid-coated nanoparticles loaded with recombinant tissue plasminogen activator for the treatment of mice with ischemic stroke, Biochem. Biophys. Res. Commun. 516 (2019) 565–570.
[19] P. Sen, M. Saha, S.S. Ghosh, Nanoparticle mediated alteration of EMT dynamics: an approach to modulate cancer therapeutics, Mater. Adv. 1 (2020) 2614–2630.
[20] S. Santra, D. Dutta, G.A. Walter, B.M. Moudgil, Fluorescent nanoparticle probes for cancer imaging, Technol. Canc. Res. Treat. 4 (2005) 593–602.
[21] G. Gul, R. Yildirim, N. Ileri-Ercan, Cytotoxicity analysis of nanoparticles by association rule mining, Environ. Sci. Nano 8 (2021) 937–949.
[22] P.G. Jeelani, P. Mulay, R. Venkat, C. Ramalingam, Multifaceted application of silica nanoparticles, A Review. *Silicon* 12 (2020) 1337–1354.
[23] A. Bitar, N.M. Ahmad, H. Fessi, A. Elaissari, Silica-based nanoparticles for biomedical applications, Drug Discov. Today 17 (2012) 1147–1154.
[24] K. Räsänen, A. Vaheri, TGF-beta1 causes epithelial-mesenchymal transition in HaCaT derivatives, but induces expression of COX-2 and migration only in benign, not in malignant keratinocytes, J. Dermatol. Sci. 58 (2010) 97–104.
[25] T. Wang, et al., TGF-β-induced miR-21 negatively regulates the antiproliferative activity but has no effect on EMT of TGF-β in HaCaT cells, Int. J. Biochem. Cell Biol. 44 (2012) 366–376.

[26] M. Sohn, et al., Ahnak promotes tumor metastasis through transforming growth factor-β-mediated epithelial-mesenchymal transition, Sci. Rep. 8 (2018) 2–11.
[27] H. Shin, M. Kwak, T.G. Lee, J.Y. Lee, Quantifying the level of nanoparticle uptake in mammalian cells using flow cytometry, Nanoscale 12 (2020) 15743–15751.
[28] J. Zhang, et al., TGF-β-induced epithelial-to-mesenchymal transition proceeds through stepwise activation of multiple feedback loops, Sci. Signal. 7 (2014) ra91.
[29] H. Kasai, J.T. Allen, R.M. Mason, T. Kamimura, Z. Zhang, TGF-β1 induces human alveolar epithelial to mesenchymal cell transition (EMT), Respir. Res. 6 (2005) 1–15.
[30] B. Baum, M. Georgiou, Dynamics of adherens junctions in epithelial establishment, maintenance, and remodeling, J. Cell Biol. 192 (2011) 907–917.
[31] S. Rafehi, et al., TGFβ signaling regulates Epithelial-mesenchymal plasticity in ovarian cancer ascites-derived spheroids, Endocr. Relat. Canc. 23 (2016) 147–159.
[32] M. Maeda, K.R. Johnson, M.J. Wheelock, Cadherin switching: essential for behavioral but not morphological changes during an epithelium-to-mesenchyme transition, J. Cell Sci. 118 (2005) 873–887.
[33] N.E. Wikner, K.A. Persichitte, J.B. Baskin, L.D. Nielsen, R.A.F. Clark, Transforming growth factor-β stimulates the expression of fibronectin by human keratinocytes, J. Invest. Dermatol. 91 (1988) 207–212.
[34] J. Park, J.E. Schwarzbauer, Mammary epithelial cell interactions with fibronectin stimulate epithelial-mesenchymal transition, Oncogene 33 (2014) 1649–1657.
[35] O. Ispanixtlahuatl-Meráz, R.P.F. Schins, Y.I. Chirino, Cell type specific cytoskeleton disruption induced by engineered nanoparticles, Environ. Sci. Nano 5 (2018) 228–245.
[36] R. Cornu, C. Chrétien, Y. Pellequer, H. Martin, A. Béduneau, Small silica nanoparticles transiently modulate the intestinal permeability by actin cytoskeleton disruption in both Caco-2 and Caco-2/HT29-MTX models, Arch. Toxicol. 94 (2020) 1191–1202.
[37] J.A. Kim, C. Aberg, A. Salvati, K.A. Dawson, Role of cell cycle on the cellular uptake and dilution of nanoparticles in a cell population, Nat. Nanotechnol. 7 (2012) 62–68.
[38] J.L. Leight, M.A. Wozniak, S. Chen, M.L. Lynch, C.S. Chen, Matrix rigidity regulates a switch between TGF-β1-induced apoptosis and epithelial-mesenchymal transition, Mol. Biol. Cell 23 (2012) 781–791.
[39] S. Liarte, Á. Bernabé-García, F.J. Nicolás, Human skin keratinocytes on sustained TGF-β stimulation reveal partial EMT features and weaken growth arrest responses, Cells 9 (2020) 1–20.
[40] S. Behzadi, et al., Cellular uptake of nanoparticles: journey inside the cell, Chem. Soc. Rev. 46 (2017) 4218–4244.
[41] J. Pu, C.M. Guardia, T. Keren-Kaplan, J.S. Bonifacino, Mechanisms and functions of lysosome positioning, J. Cell Sci. 129 (2016) 4329–4339.
[42] T.C. Rao, et al., EGFR activation attenuates the mechanical threshold for integrin tension and focal adhesion formation, J. Cell Sci. 133 (2020).
[43] M. Karakozova, et al., Arginylation of b-actin regulates actin cytoskeleton and cell motility, Science 313 (2006) 192–196.